Thermodynamic and transport properties of the one-dimensional $S=\frac{1}{2}$ antiferromagnet Yb_4As_3

P. Gegenwart[a,*], H. Aoki[a], T. Cichorek[a], J. Custers[a], N. Harrison[b], M. Jaime[b], M. Lang[c], A. Ochiai[d], F. Steglich[a]

[a] *Max-Planck Institute for Chemical Physics of Solids, Noethnitzer Str. 48, D-01187 Dresden, Germany*
[b] *Los Alamos National Laboratory, Los Alamos, New Mexico 87545, USA*
[c] *Institute for Physics, University of Frankfurt, 60054 Frankfurt (Main), Germany*
[d] *Center for Low Temperature Science, Tohoku University, Sendai 980-8578, Japan*

Abstract

The semimetallic quasi-one-dimensional $S=\frac{1}{2}$ antiferromagnet Yb_4As_3 has been studied by performing low-temperature (T) and high magnetic-field (B) measurements of the specific heat, $C(T,B)$, magnetization, $M(T,B)$, AC-susceptibility, $\chi_{AC}(T,B)$, and electrical resistivity, $\rho(T,B)$. At finite transverse magnetic fields, a gap $\Delta(B)$ is induced in the low-energy magnetic excitation spectrum. Our $C(T,B)$ measurements reveal a $\Delta(B)\sim B^{2/3}$ dependence for $B\leqslant 9\,\mathrm{T}$, in accordance with predictions of the quantum sine-Gordon model. At higher fields the $\Delta(B)$ curve levels-off gradually. In the isothermal magnetization taken at 0.6 K no saturation occurs up to 60 T. We also present new results on spin-glass behavior below 0.15 K caused by a weak ferromagnetic interchain coupling and disorder. Finally, we concentrate on the electrical transport properties. Shubnikov-de Haas oscillations, arising from a low-density system of mobile As-4p holes, are recorded in magnetic fields up to 60 T. We estimate the effective mass and the mean-free path of these carriers and discuss spin-splitting effects.

Keywords: Yb_4As_3; One-dimensional Heisenberg chain; Spin glass; Shubnikov-de Haas effect

1. Introduction

Quasi-one-dimensional (1D) quantum magnets have been in the focus of intense theoretical and experimental interest for a long time. Antiferromagnetic (AF) $S=\frac{1}{2}$ Heisenberg chains show gapless two-spinon continuum (or "magnon") excitations as described by des Cloizeaux and Pearson [1]. A recently studied example is the organic compound Cu-benzoate for which a magnon-derived linear in-T dependence of the low-temperature specific heat has been observed at zero magnetic fields, $B=0$ [2]. B-fields that transverse to the Cu^{2+} ($S=\frac{1}{2}$)-chain direction induce a gap in the low-energy excitations observed by both inelastic-neutron diffraction and specific-heat experiments [2]. This result is not expected for an AF $S=\frac{1}{2}$ Heisenberg chain, but was explained within the frame of the quantum sine-Gordon (SG) theory, taking into account a staggered field perpendicular to the chains [3]. While in the insulating Cu-benzoate the spin chains are dictated by the crystal structure at all temperatures, in the rare-earth pnictide compound Yb_4As_3 it is a charge-ordering (CO) transition near room temperature [4] which leads to the formation of 1D spin chains at lower T. At high temperature, in the cubic phase, Yb_4As_3 is an intermediate-valence metal with an average valence ratio $Yb^{3+}/Yb^{2+}=1{:}3$. The Yb ions are located on the four interpenetrating families of the cubic space diagonals. At $T_{CO}\approx 295\,\mathrm{K}$, driven by intersite Coulomb interactions and a deformation potential coupling to the lattice, the smaller Yb^{3+} ions order along one of the cubic space diagonals. The trigonal lattice distortion accompanying

*Corresponding author. Tel.: +49-351-4646-2324; fax: +49-351-4646-2360.
E-mail address: gegenwart@cpfs.mpg.de (P. Gegenwart).

the CO transition usually results in the formation of a polydomain low-T structure. A preferential orientation of the domains can be induced by the application of a small uniaxial pressure along one space diagonal prior to cooling through T_{CO}. The crystal-electric field (CEF) ground state of the Yb^{3+} ions can be described by an effective $S=\frac{1}{2}$ doublet [5]. The Yb^{3+} chains are well separated from each other by nonmagnetic Yb^{2+} and As ions. The low-energy excitations of these $S=\frac{1}{2}$ chains have been found using inelastic neutron-scattering (INS) experiments [5] to agree well with the des Cloizeaux–Pearson spectrum of a 1D $S=\frac{1}{2}$ Heisenberg AF with a nearest-neighbor AF coupling $|J|=2.2\,\mathrm{meV}$ (corresponding to $k_B \cdot 25.5\,\mathrm{K}$). Very recently, Shiba et al. [6] showed theoretically that the zero-field ground-state Hamiltonian of the CO variant of Yb_4As_3 can be mapped onto the 1D *isotropic* $S=\frac{1}{2}$ Heisenberg AF. The large heavy-fermion (HF)-like in-T linear contribution to the specific heat, γT, with $\gamma=0.2\,\mathrm{J/K^2\,mol}$ [7] is in excellent agreement with the expected "magnon" contribution. In the following we consider the CO state of Yb_4As_3 as a model system for studying the low-lying excitations of AF $S=\frac{1}{2}$ chains *despite* the presence of a small number of intrinsic charge carriers.

The paper is organized as follows: After giving details concerning experimental techniques in Section 2, we address in Section 3 the effect of applying transverse magnetic fields to the spin chains. Pulsed-field (60 T) magnetoresistivity and magnetization as well as specific-heat experiments up to 18 T are discussed and compared with recent INS experiments [8] and the theoretical prediction of the quantum sine-Gordon model [9]. In Section 4 we present new results concerning spin-glass behavior at very low temperature caused by weak interchain coupling and disorder. Finally, we address the electrical transport in Yb_4As_3 and give a quantitative analysis of Shubnikov-de Haas (SdH) oscillations observed in the isothermal resistivity (Section 5). The conclusions are presented in Section 6.

2. Experimental details

The experiments were carried out using high-quality single crystals as described in Ref. [4]. For the specific heat and DC-magnetization measurements, a microcalorimeter from Oxford Instruments and a quantum design SQUID magnetometer were used, respectively. The low-T AC-susceptibility and resistivity were measured by conducting a low-frequency lock-in technique adapted to a $^3He/^4He$ dilution refrigerator. High-field experiments were performed in the Los Alamos High Magnetic Field Laboratory using a short pulse (25 ms) 60 T magnet.

3. Field-induced gap

In the following, we discuss the effect of external magnetic fields applied to the AF $S=\frac{1}{2}$ chains. Upon increasing the field, $C(T)/T$ becomes progressively reduced below 1 K, while at somewhat higher temperatures a broad hump forms which is shifted with increasing B continuously towards higher T [7]. This suggests the opening of a gap in the low-energy excitation spectrum. By a detailed analysis of corresponding anomalies found in the thermal expansion $\alpha(T,B)$ experiments, where by the application of small uniaxial pressure in domain configuration was varied deliberately, it was shown that a *finite*-field component perpendicular to the short axis (i.e. the $S=\frac{1}{2}$ chains) is required to induce the anomaly [10]. Several scenarios have been proposed to account for these observations: (i) a very weak interchain coupling [11], (ii) an intrachain dipolar interaction [12], and (iii) solitary excitations described by the *classical* sine-Gordon solution of a 1D Heisenberg AF with a weak easy-plane anisotropy and, in addition, a weak interchain coupling [10]. Within the latter model, the observed minima in the thermal conductivity $\kappa(B)/\kappa(0)$ are also explained quite naturally assuming a resonant scattering of the three-dimensional phonons by the magnetic solitons [10]. Since the *quantum* sine-Gordon theory can only be applied to the low-T specific heat [9], the *classical* sine-Gordon model as described above had to be used to describe the bumps in $C(T)/T$ as well as the extrema in the T-dependencies of both the thermal expansion and the thermal conductivity, which occur at elevated temperatures. This yielded excellent fits to the data for all three

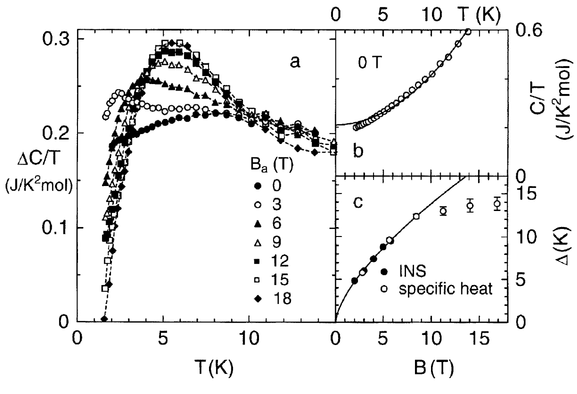

Fig. 1. Specific heat $C(T)/T$ at varying magnetic fields B_a applied along the cubic $\langle 111 \rangle$ direction of polydomain Yb_4As_3. (a) $\Delta C/T$ denote values after subtraction of phonon contribution $C_{ph}/T=\gamma+\beta T^2$ using $\gamma=0.21\,\mathrm{J/K^2\,mol}$ and $\beta=2.05\times10^{-3}\,\mathrm{J/K^4\,mol}$ indicated by a solid line in (b). (c) Spin-excitation gap Δ as derived from inelastic-neutron scattering (INS) [8] and specific heat data (see text).

quantities by allowing for three adjustable parameters in each case [10]. The limitation of the *classical* sine-Gordon model, however, became evident when the field dependence of one of the common fit parameters, the soliton rest energy, E_s, was determined and observed to obey a power-law dependence: $E_s \sim B^{\nu}$. In contrast to the prediction of the *classical* model, $\nu = 1$, however, $\nu \approx 2/3$ was found to describe the results of the $C(T, B)$, $\alpha(T, B)$ and $\kappa(T, B)$ experiments satisfactorily well. Since a $B^{2/3}$ law is predicted by the *quantum* sine-Gordon theory for the field dependence of the spin gap it was concluded [13] that in a quantum-spin system, the gap and the soliton rest energy have the same origin, while they are independent of each other in the classical model.

The quantum sine-Gordon theory was applied to Yb_4As_3 by Oshikawa et al. [9] and Shiba et al. [6]. They showed that the absence of a center of inversion between two adjacent Yb^{3+} ions along the chain due to an alternating surrounding of As ions gives rise to a Dzyaloshinskii-Moriya (DM) interaction. The glide reflection with the glide vector parallel to the Yb^{3+} chains requires an alternating sign for the DM interaction. An external field with a component perpendicular to the spin-chain direction therefore produces a staggered field. According to Ref. [9] the staggered field induces an excitation gap $\Delta \sim |J|^{1/3} B^{2/3}$, where B is the perpendicular component of the applied field B_a with respect to the spin chain. Recent INS measurements in $B \leqslant 5.8\,\mathrm{T}$ revealed that the spectrum at the 1D wave vector $\boldsymbol{q}$ with $|\boldsymbol{q}| = \pi/d$ changes drastically from the lower bound of the (two)-spinon continuum found in zero field to a sharp one at finite energy, indicating the opening of an energy gap [8]. The derived $\Delta(B)$ curve follows the predicted $B^{2/3}$ dependence (see Fig. 1c).

Here we report on heat-capacity experiments in high magnetic fields which allow us to follow the $\Delta(B)$ dependence up to higher B. We have studied a polydomain sample in magnetic fields oriented parallel to one of the four equivalent cubic space diagonals. Therefore, below the CO transition, about 25% of the domains are oriented with the spin chains parallel to the applied field B_a and about 75% of the domains are aligned such that the effective field component perpendicular to the spin chains is $B = B_a \sin(70°)$. Since for the former volume fraction no staggered field is induced, the field dependence observed in Fig. 1 is due to the latter.

$C_{ph} = \beta T^3$ with $\beta = 2.05 \times 10^{-3}\,\mathrm{J/K^4\,mol}$ which was obtained from the zero-field measurement (Fig. 1b). The remaining $\Delta C/T = C(T, B)/T - C_{ph}/T$ shows maxima corresponding to those observed in thermal expansion [10] whose position shifts to higher T with increasing fields for $B_a \leqslant 12\,\mathrm{T}$ and saturates for higher B. This result is very different to the prediction of a recent calculation of the specific heat of monodomain Yb_4As_3 for elevated T and transverse magnetic fields up to 24 T

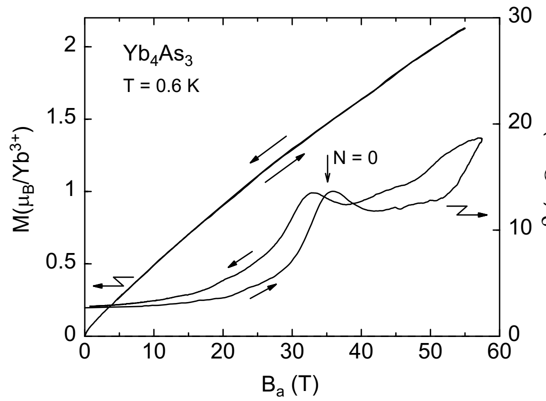

Fig. 2. Pulsed-field DC-magnetization (left axis) and transverse magnetoresistivity (right axis) at 0.6 K for B_a applied along the cubic $\langle 1\,1\,1 \rangle$ direction of polydomain Yb_4As_3. Arrows indicate magnetic history and calculated position of the SdH maximum corresponding to the Landau quantum number $N = 0$ (see text).

using the finite-T density-matrix renormalization-group method by Shibata and Ueda [14]. According to their exact calculation, the result of the quantum sine-Gordon model, that the maxima in $\Delta C/T$ are located at about 0.4Δ, is roughly valid up to 24 T which allows us to determine the $\Delta(B)$ dependence (within 15% error) from our heat-capacity data. As shown in Fig. 1c, $\Delta(B)$ follows the predicted $B^{2/3}$ dependence up to 9 T. Upon increasing B further, the Zeeman energy becomes comparable to the intrachain coupling. This leads to the destruction of the 1D AF state, and a crossover to a ferromagnetic polarization of the spins occurs, accompanied by a flattening of the $\Delta(B)$ dependence. According to Uimin et al. [12], the excitation gap even disappears at a transverse field $g_{\perp}\mu_B B/J \geqslant 2$ which corresponds, using the g-value $g_{\perp} = 1.2$ determined by polarized-neutron diffraction [15], to $B \geqslant 67\,\mathrm{T}$. To obtain further information on the high-field behavior of Yb_4As_3, we have performed pulsed-field experiments of $M_{dc}(B)$ and $\rho(B)$ at very low temperatures (0.6 K) and up to 60 T applied along the cubic $\langle 1\,1\,1 \rangle$ direction of our polydomain crystals. As shown in Fig. 2, $M_{dc}(B)$ shows a monotonic behavior without any indication for saturation or an additional anomaly. However, $M_{dc}(B)$ should be strongly affected by the single-ion CEF excitations. Therefore, besides the contribution of the 1D-spin chains, a large Van Vleck-type contribution is expected which should not saturate up to very high magnetic fields since the highest CEF excitation of the $J = \frac{7}{2}$ multiplet is located at 29 meV corresponding to a magnetic field of roughly 400 T. The isothermal resistivity $\rho(B)$ is not affected by the magnetic degrees of freedom of the Yb^{3+} chains and the distinct anomalies are due to the extremely low carrier concentration (see below).

4. Interchain coupling and low-T spin-glass freezing

Using a small uniaxial-pressure cell to induce a monodomain crystal in the CO state, Aoki et al. found an intrinsic upturn in the low-T susceptibility, even for magnetic fields applied parallel to the spin chains [16] which, therefore, cannot be explained by the staggered-field model and must be caused by a weak ferromagnetic interchain coupling [17,18].

To investigate the susceptibility of Yb_4As_3 at sufficiently low temperatures, where interchain-coupling effects become important, we measured the ac-susceptibility χ_{ac}. The absolute values of χ_{ac} have been determined from a comparison in the temperature range $2\,K \leqslant T \leqslant 6\,K$ with the results of the dc-susceptibility measured in 50 mT using the SQUID magnetometer [19]. At $T = 0.12\,K$, spin-glass (SG) freezing is observed with the characteristic high sensitivity to small superimposed dc-fields (Fig. 3a). The relative shift $\delta = \Delta T_f/(\Delta \log(2\pi\nu)T_f)$ of the freezing temperature T_f per decade in the frequency of the ac-field, ν, is estimated as $\delta = 0.03 \pm 0.005$, i.e. a value between that found for metallic and insulating spin-glasses (Fig. 3b) [20]. A uniaxial-pressure experiment of the low-T ac-susceptibility showed that the SG freezing is not affected by domain disorder [21]. The *antiferromagnetic* intrachain coupling together with the weak *ferromagnetic* interchain coupling leads to frustration along the chains. Taken together with the disorder that is present on the Yb^{3+}-chains inferred, e.g. from the relative short carrier mean-free path obtained from SdH experiments as described below, the SG-freezing effects can be understood quite naturally.

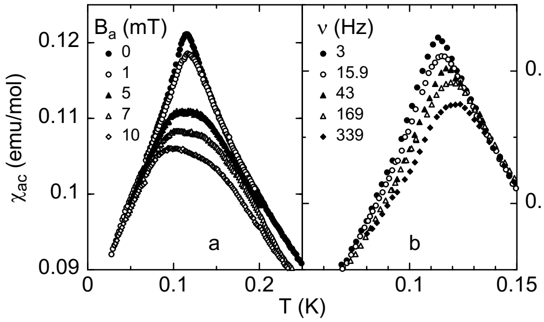

Fig. 3. Temperature dependence of the ac-susceptibility ($B_{ac} = 0.1\,mT$) in different fields B_a applied along the cubic $\langle 1\,1\,1 \rangle$ direction of polydomain Yb_4As_3 (a) and taken at different frequencies ν (b) in $B_a = 0$.

5. Resistivity and Shubnikov-de Haas effect

In the CO state, Yb_4As_3 is a compensated semimetal, with 3D charge carriers: the number of light and mobile As-4p holes exactly equals the number of heavy Yb-4f electrons in the partially filled 4f hole level [23]. Most remarkably, the electrical resistivity $\rho(T)$ shows typical HF-like behavior [4], i.e. a $\rho(T) - \rho_0 = aT^2$ dependence between 4 and 20 K with a huge coefficient a (Fig. 4a). However, due to the low-carrier concentration of the order of 10^{-3}/f.u. [4], the usual Kondo-scenario underlying HF physics can be excluded. Interestingly enough, the large coefficient a remains almost unchanged up to 18 T [19], while the specific-heat coefficient γ rapidly decreases due to the gap formation [7]. This strongly suggests that it is the scattering of the light and mobile As-4p holes by the heavy Yb-4f electrons as opposed to scattering by the magnon-like excitations (cf. Ref. [23]) that leads to the large coefficient a in resistivity. At lower temperatures, $\rho(T)$ deviates from the T^2 behavior, passes through a minimum at 2 K followed by a 0.15% increase and saturation below 0.1 K (Fig. 4b). The increase of the low-T resistivity is very probably related to the SG effects. The isothermal resistivity (Fig. 4c) roughly follows a B^2 behavior with superimposed SdH oscillations as has also been observed by Aoki et al. [22]. According to LSDA + U band-structure calculations, both the hole and electron sheets of the Fermi surface are almost spherical [23]. We expect the SdH oscillations to arise from the light As-4p holes since their mobility is much larger than that of the much heavier Yb-4f electrons. In the magnetic-field interval $B = 4.5 - 12\,T$, an SdH frequency $f = 25\,T$ is found similar as reported in [22]. The oscillations result from

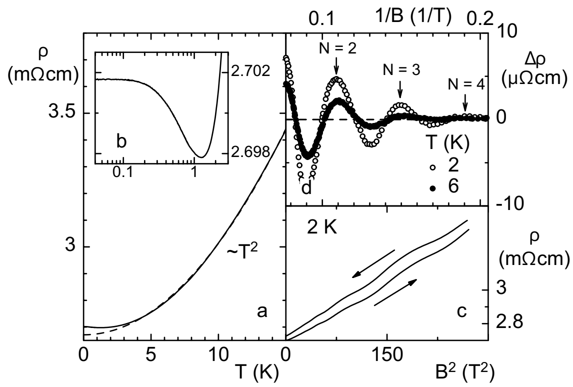

Fig. 4. Electrical resistivity for polydomain Yb_4As_3, plotted as ρ vs. T (a), ρ vs. $\log(T/K)$ (b), and ρ vs. B^2 (c). The dashed line in (a) represents $\Delta\rho(T) = 3.4\,\mu\Omega\,cm/K^2\,T^2$, the arrows in (c) indicate magnetic history of the data. The vertical shift in (c) is due to relaxation. (d): SdH oscillations at two different temperatures. Arrows indicate Landau quantum numbers N of the observed maxima in the SdH effect.

the depopulation of the Landau tubes $N = 4$, 3 and 2 (Fig. 4d). Assuming one pair of As-4p bands as derived from LSDA + U band-structure calculations [23], the observed frequency of 25 T would correspond to a carrier concentration $n \approx 1.4 \times 10^{18}\,\mathrm{cm}^{-3}$, whereas the low-$T$ Hall coefficient R_H determined on the same single crystal reveals a two times larger value of $(eR_H)^{-1} \approx 3 \times 10^{18}\,\mathrm{cm}^{-3}$ [18]. The reason for this discrepancy is unclear yet and needs further theoretical investigations.

For $B \geqslant 12.5$ T additional oscillations are observed, which might be related to spin splitting because of the extremely low-carrier concentration, the system is already in the quantum limit. Assuming a splitting $v_s = 0.016\,\mathrm{T}^{-1}$ of the $N = 1$ maximum (see dotted lines in Fig. 5), the effective Landé g-factor for the As-4p holes given by $g_{\mathrm{eff}} = 2v_s f/(m_{\mathrm{eff}}/m_0)$ is calculated as 2.9 ± 0.2. Here we used the effective carrier mass $m_{\mathrm{eff}} = (0.275 \pm 0.005)m_0$ determined from the analysis of the T-dependence of the SdH oscillations in low fields (Fig. 6a). It is difficult to analyze the several additional oscillations in the SdH effect found for $B \geqslant 20$ T (Fig. 5), except for a pronounced peak in $\rho(B)$ developing around 35 T: at this field, the SdH maximum related to $N = 0$ should appear (see Fig. 2).

The analysis of the field dependence of the oscillations below 8.5 T taken at differing temperatures, reveals a Dingle temperature of $T_D = 6.6$ K corresponding to a charge-carrier mean-free path of ≈ 215 Å. We note that the magnon mean-free path along the $S = \frac{1}{2}$ chains determined from the $B = 0$ thermal conductivity is roughly 500 Å [18], and that both values are much smaller than the domain size of approximately 1 μm.

Finally, we address the pronounced hysteresis of the electrical resistivity upon increasing and decreasing B (Figs. 2 and 4c and Inset Fig. 5) as well as upon warming and cooling in $B > 0$ [19]. To further study this effect which was also observed on a monodomain single crystal [19], we recorded the time-dependence of the resistivity $\rho(t)$ after the application of 16.5 T over 10 h at several temperatures below 7 K (Fig. 7). A pronounced relaxation was found which does not saturate after 10 h and cannot be fitted to a simple logarithmic decay. This relaxation effect increases with decreasing T, reaching about 1.5‰ at 2 K. The origin of the hysteresis loop and relaxation in the resistivity has been unclear until now. It might be related to a slow motion of static point defects: No corresponding hysteresis was found in the dc-magnetization $M(B)$ (Fig. 2) and no relaxation larger than 0.1‰ at 2 K was observed in $M(t)$, measured by using a SQUID magnetometer after the application of 7 T [24].

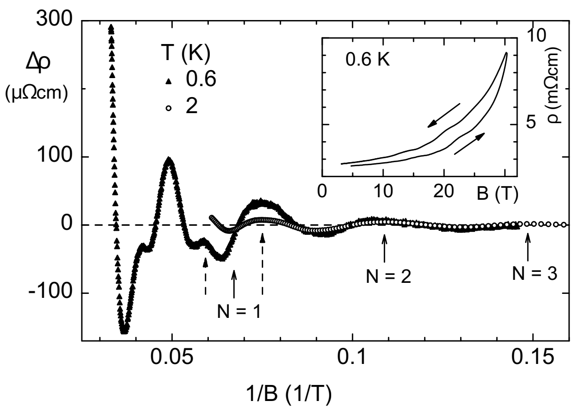

Fig. 5. SdH oscillations for Yb_4As_3, obtained at 2 K from the data shown in Fig. 4c and at 0.6 K from pulsed-field data shown in the inset. Landau quantum numbers N are indicated by arrows. Spin splitting of $N = 1$ orbit is indicated by dotted lines.

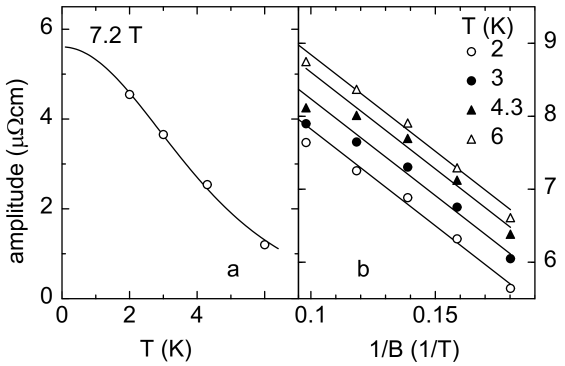

Fig. 6. (a) T-dependence of the SdH oscillations at 7.2 T (symbols) and a fit to the standard Lifshitz and Kosevich theory (solid line). (b) Dingle-plot of log(amplitude $\cdot B^{1/2} \sinh(14.69\,\mathrm{T/K}\, m^*/m_0\, T/B)$) vs. $1/B$. From the slope of the solid lines a Dingle temperature of $T_D = 6.6$ K is estimated.

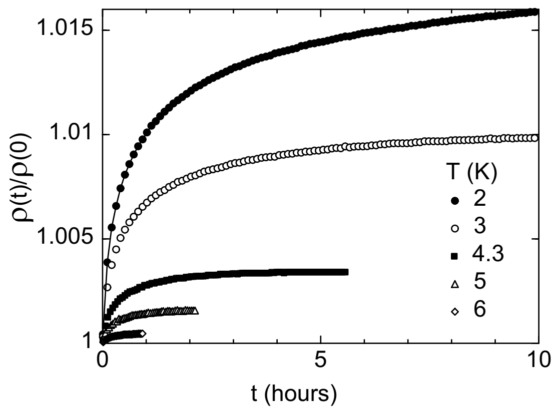

Fig. 7. Relaxation of the electrical resistivity in $B = 16.5$ T (applied with a rate of 0.25 T/min), plotted as $\rho(t)/\rho(0)$ vs. time, t, at different temperatures.

6. Conclusion

We have presented new thermodynamic and transport experiments on the low-carrier density $S=\frac{1}{2}$ antiferromagnet Yb_4As_3. Finite transverse magnetic fields (i) open a gap $\Delta(B)$ in the low-energy excitations and (ii) lead to soliton-like anomalies in thermodynamic properties and the phonon thermal conductivity. These two types of phenomena are not independent of, but are closely related to each other. The magnetic-field dependence of $\Delta(B)$ was found to follow the $B^{2/3}$ dependence predicted by the quantum-sine-Gordon model for $B \leqslant 9\,T$. At higher fields, $\Delta(B)$ levels-off gradually. In the dc-magnetization no indication for a phase transition is observed up to 60 T. Disorder, together with a weak ferromagnetic coupling between the AF chains, leads to a low-T SG transition at 0.12 K. The transport properties, arising from the 3D semimetallic character of Yb_4As_3, were investigated down to very low temperatures ($T \geqslant 20\,mK$) and up to very high magnetic fields ($B \leqslant 60\,T$). A detailed analysis of the SdH oscillations confirms the existence of a small concentration of light As-4p holes. The HF-like resistivity observed even in high magnetic fields where the large $B=0$ in-T linear specific heat is suppressed, suggests a two-band model of current-carrying As-derived 4p-holes scattered by heavy Yb-derived 4f electrons.

Acknowledgements

We gratefully acknowledge stimulating discussions with M. Kohgi, K. Iwasa, T. Suzuki, B. Schmidt, P. Thalmeier, A. Yaresko, N. Shibata and K. Ueda.

References

[1] J. des Cloizeaux, J.J. Pearson, Phys. Rev. 128 (1962) 2131.
[2] D.C. Dender, P.R. Hammar, D.N. Reich, C. Broholm, G. Aeppli, Phys. Rev. Lett. 79 (1997) 1750.
[3] M. Oshikawa, I. Affleck, Phys. Rev. Lett. 79 (1997) 2883.
[4] A. Ochiai, T. Suzuki, T. Kasuya, J. Phys. Soc. Japan 59 (1990) 4129.
[5] M. Kohgi, K. Iwasa, J.-M. Mignot, A. Ochiai, T. Suzuki, Phys. Rev. B 56 (1997) R11388.
[6] H. Shiba, K. Ueda, O. Sakai, J. Phys. Soc. Japan 69 (2000) 1493.
[7] R. Helfrich, M. Köppen, M. Lang, F. Steglich, A. Ochiai, J. Magn. Magn. Mater. 177–181 (1998) 309.
[8] M. Kohgi, K. Iwasa, J.-M. Mignot, B. Fåk, P. Gegenwart, M. Lang, A. Ochiai, H. Aoki, T. Suzuki, Phys. Rev. Lett. 86 (2001) 2439.
[9] M. Oshikawa, K. Ueda, H. Aoki, A. Ochiai, M. Kohgi, J. Phys. Soc. Japan 68 (1999) 3181.
[10] M. Köppen, M. Lang, R. Helfrich, F. Steglich, P. Thalmeier, B. Schmidt, B. Wand, D. Pankert, H. Benner, H. Aoki, A. Ochiai, Phys. Rev. Lett. 82 (1999) 4548.
[11] B. Schmidt, P. Thalmeier, P. Fulde, Europhys. Lett. 35 (1996) 109.
[12] G. Uimin, Y. Kudasov, P. Fulde, A. Ovchinnikov, Eur. Phys. J. B 16 (2000) 241.
[13] F. Stegich, M. Köppen, P. Gegenwart, T. Cichorek, B. Wand, M. Lang, P. Thalmeier, B. Schmidt, H. Aoki, A. Ochiai, Acta Phys. Pol. 97 (2000) 91.
[14] N. Shibata, K. Ueda, J. Phys. Soc. Jpn. 70 (2001) 3690.
[15] K. Iwasa, M. Kohgi, A. Gukasov, J.-M. Mignot, N. Shibata, A. Ochiai, H. Aoki, T. Suzuki, J. Magn. Magn. Mater. 226–230 (2001) 441.
[16] H. Aoki, A. Ochiai, M. Oshikawa, K. Ueda, Physica B 281&282 (2000) 465.
[17] H. Aoki, Ph.D. Thesis, Tohoku University, 2000, unpublished.
[18] B. Schmidt, H. Aoki, T. Cichorek, J. Custers, P. Gegenwart, M. Kohgi, M. Lang, C. Langhammer, A. Ochiai, S. Paschen, F. Steglich, T. Suzuki, P. Thalmeier, B. Wand, A. Yaresko, Phys. B 300 (2001) 121.
[19] P. Gegenwart, T. Cichorek, J. Custers, M. Lang, H. Aoki, A. Ochiai, F. Steglich, J. Magn. Magn. Mater. 226–230 (2001) 630.
[20] J. Mydosh, Spin Glasses: an Experimental Introduction, Taylor & Francis, London, Washington DC, 1993.
[21] P. Gegenwart, et al., to be published.
[22] H. Aoki, A. Ochiai, N. Kimura, T. Terashima, C. Terakura, H. Harima, J. Phys. Soc. Jpn., submitted.
[23] V.N. Antonov, A.N. Yaresko, A.Ya. Perlov, P. Thalmeier, P. Fulde, P.M. Oppeneer, H. Eschrig, Phys. Rev. B 58 (1998) 975.
[24] P. Gegenwart, H. Aoki, T. Cichorek, J. Custers, M. Jaime, A. Ochiai, F. Steglich, Pramana-J. Phys., submitted.